Mathematics and Computers in Simulation 249 (2026) 1041–1056

Contents lists available at ScienceDirect

Mathematics and Computers in Simulation

journal homepage: www.elsevier.com/locate/matcom

Original articles

Simplex-splines on the Clough–Tocher split for high-order numerical approximation ☆

Jean-Louis Merrien [a], Francesca Pelosi [b],*, Maria Lucia Sampoli [b], Hendrik Speleers [c]

[a] University of Rennes, INSA Rennes, CNRS, IRMAR - UMR 6625, France
[b] University of Siena, Department of Information Engineering and Mathematics, Italy
[c] University of Rome Tor Vergata, Department of Mathematics, Italy

ARTICLE INFO

MSC:
41A15
65D07
65N30

Keywords:
Triangulations
Piecewise polynomials
Simplex-splines
Numerical approximation

ABSTRACT

Smooth splines defined on (possibly refined) triangulations are widely used in the area of data fitting and numerical analysis of partial differential equations, in particular isogeometric analysis. A classical choice is the C^1 cubic spline space defined on the Clough–Tocher split, which divides each triangle into three subtriangles by connecting the barycenter of the triangle to its three vertices. In this paper, we consider the more general family of C^1 spline spaces of degree $d \geq 3$. Recently, a simplex-spline basis was developed with the aim of having an effective local representation of such splines on each triangle. Here we investigate the use of these (local) simplex-splines as a practical tool to build C^1 spline approximations over general triangulations and numerically test them in the least-squares method for function approximation and in the Galerkin method for solving linear and semilinear elliptic problems.

1. Introduction

Classical univariate B-splines and their rational extension NURBS have been well studied and widely used in today's industrial applications due to their superior capability of representing both free-form and common analytical shapes. Their bivariate generalizations have also found many applications in the area of data fitting, geometric shape modeling, and numerical analysis of partial differential equations. These bivariate generalizations can be classified into tensor-product splines and non-tensor-product splines; see, e.g., [1,2]. The main advantages of tensor-product B-splines/NURBS are their easy implementation and computational efficiency, regardless of the dimensionality of the problem. Unfortunately, the tensor-product structure has also few drawbacks. First of all, (single-patch) NURBS lack an adequate local refinement. Furthermore, tensor-product surfaces are restricted to four-sided domains and thus have difficulty in modeling shapes with arbitrary topology. Although algorithm-wise complicated, non-tensor-product splines provide alternative powerful tools in modeling complex shapes and approximating scattered data and irregular functions.

Isogeometric Analysis (IgA) is a technology created about two decades ago with the aim to bridge the gap between Computer Aided Design (CAD) and Finite Element Analysis (FEA). The key concept in IgA is the use of the same basis functions both for the geometry descriptions (usually coming from CAD systems) and for the approximation of field variables [3,4]. The isogeometric

☆ This article is part of a Special issue entitled: 'MATCOM_MACMAS 2025' published in Mathematics and Computers in Simulation.

* Corresponding author.
E-mail addresses: jmerrien@insa-rennes.fr (J.-L. Merrien), francesca.pelosi@unisi.it (F. Pelosi), marialucia.sampoli@unisi.it (M.L. Sampoli), speleers@mat.uniroma2.it (H. Speleers).

https://doi.org/10.1016/j.matcom.2026.06.017
Received 16 October 2025; Received in revised form 14 April 2026; Accepted 14 June 2026
Available online 20 June 2026

framework results in some important advantages. In particular, it effectively mitigates geometric approximation errors, even on coarse meshes, and the high smoothness of the standard (spline) primitives in CAD systems has a beneficial impact on the whole approximation process, leading to a high accuracy per degree-of-freedom and excellent spectral properties [5,6]. The initial investigations of IgA focused on tensor-product B-splines/NURBS due to their dominance in industrial CAD systems. Later, to deal with complex topologies and allow for adaptive refinement, several B-spline extensions have been introduced, including T-splines [7,8], truncated hierarchical B-splines [9,10], and LR-splines [11,12]. However, due to their (local) tensor-product structures, there are still restrictions on the refinement. For example, local refinement of T-splines generally propagates beyond the region of interest.

FEA mainly utilizes piecewise functions defined on triangulations, thus smooth splines over triangulations can be an interesting tool. Compared with tensor-product structures, the use of triangulations for tiling the domain offers more flexibility in describing the geometry and performing local refinement. However, this comes at the expense of more complicated constructions of the spaces. To achieve C^1 smoothness on an arbitrary triangulation with a local construction, quintic polynomials on each triangle are required [13]. A possible way to overcome this problem is to refine the given triangulation into a finer triangulation by splitting every triangle. The best-known examples are the Clough–Tocher and Powell–Sabin splits, which divide every triangle into three and six subtriangles, respectively (see, e.g., [13]). In the context of FEA and IgA, the potential of smooth spline spaces over triangulations has been tested in several papers; see, e.g., [14–18] and references therein.

The Bernstein–Bézier form is the most popular method for the construction and analysis of smooth spline spaces over (refined) triangulations; see, e.g., [13,19]. Recently, also simplex-spline techniques have been applied to this purpose; see, e.g., [20,21]. In [22], a simplex-spline basis was constructed for the C^1 cubic spline space defined on the Clough–Tocher split and this construction has been extended in [23] to any spatial dimension s and any spline degree $d \geq s+1$. The aim of the present work is to investigate the use of the latter (local) simplex-splines as a suitable approximation tool over general triangulations for $s = 2$ and $d \geq 3$. We numerically test them in the least-squares method for function approximation and in the Galerkin method for solving linear and semilinear elliptic problems. Alternative finite element constructions on the Clough–Tocher split can be found in [14,24–27].

The remainder of the paper is organized as follows. In Section 2, we recapitulate the simplex-spline basis for the C^1 spline space of degree $d \geq 3$ on the Clough–Tocher split of a triangle, proposed in [23]. In Section 3, we discuss the C^1 connection between adjacent triangles and how the corresponding smoothness conditions can be used to build a global basis for the C^1 spline space of degree d over a general triangulation. The considered space contains the polynomial space of degree d and has optimal approximation power. These properties are confirmed in Section 4 with a selection of numerical examples where we study the error on different triangulations. We end in Section 5 with some concluding remarks.

2. The tools on a triangle

In this section, we start by reviewing a recursive construction of bivariate simplex-splines and some of their properties such as differentiation. For more details on simplex-splines, we refer the reader to [2,28]. Then, we summarize from [23] the definition of a C^1 spline representation of degree $d \geq 3$ on a triangle refined by the Clough–Tocher split [25]. The special case $d = 3$ can also be found in [22].

2.1. Bivariate simplex-splines

We synopsize the definition and some properties of bivariate simplex-splines. Let us consider a set of knots in $\mathbb{R}^2$,

$$\Xi := \{\xi_0, \dots, \xi_n\}.$$

We say that a knot has multiplicity m if it occurs m times in Ξ. A line segment connecting two distinct knots is called a knot line. We denote by $\langle \Xi \rangle$ the convex hull of Ξ and by $A(\langle \Xi \rangle)$ its area.

For $n = 2$, the degree zero simplex-spline is defined by

$$M_\Xi(\boldsymbol{x}) := \begin{cases} 1/A(\langle \Xi \rangle), & \text{if } \boldsymbol{x} \in \text{interior of } \langle \Xi \rangle, \\ 0, & \text{if } \boldsymbol{x} \notin \langle \Xi \rangle. \end{cases}$$

The value of M_Ξ on the boundary of $\langle \Xi \rangle$ has to be dealt with separately. Then we use a recursion. For any $\boldsymbol{x} \in \mathbb{R}^2$ and any $b_0, \dots, b_n$ such that $\sum_{i=0}^n b_i \xi_i = \boldsymbol{x}$, $\sum_{i=0}^n b_i = 1$, we have

$$M_\Xi(\boldsymbol{x}) := \frac{n}{n-2} \sum_{i=0}^{n} b_i M_{[\Xi \setminus \xi_i]}(\boldsymbol{x}).$$

In general, M_Ξ has the following properties:

- **Nonnegativity and normalization:** M_Ξ is nonnegative and has unit integral.
- **Compact support:** M_Ξ has support $\langle \Xi \rangle$.
- **Piecewise polynomial:** M_Ξ is a polynomial of total degree $d := n-2$ on each polygon in the partition of $\langle \Xi \rangle$ formed by the knot lines.
- **Smoothness:** Across a knot line, we have $M_\Xi \in C^{n-1-\mu}$, where μ is the number of knots in the affine hull of the knot line, including multiplicities.

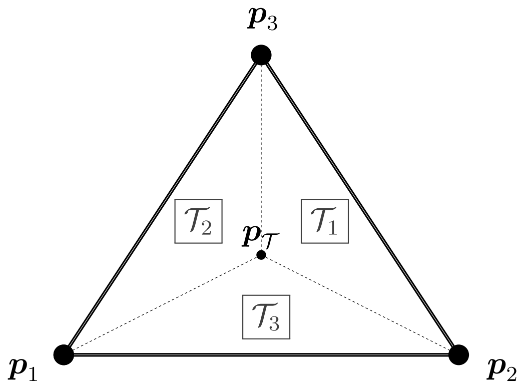

Fig. 1. The Clough–Tocher split $\mathcal{T}_{\mathrm{CT}}$ of a triangle $\mathcal{T}$ and the corresponding notation.

- **Differentiation formula:** For any $\boldsymbol{u} \in \mathbb{R}^2$ and any $a_0, \ldots, a_n$ such that $\sum_{i=0}^n a_i \xi_i = \boldsymbol{u}$, $\sum_{i=0}^n a_i = 0$, we have

$$(\boldsymbol{u} \cdot \nabla) M_{\Xi} = n \sum_{i=0}^{n} a_i M_{[\Xi \setminus \xi_i]},$$

where ∇ denotes the gradient.

If Ξ only consists of three distinct points, say $\{\boldsymbol{\eta}_1, \boldsymbol{\eta}_2, \boldsymbol{\eta}_3\}$, with multiplicity $\{m_1, m_2, m_3\}$, then M_{Ξ} is a pure polynomial of degree $n-2$ on $\langle \Xi \rangle$. Note that in this case we have $\Xi = \{\xi_0, \ldots, \xi_n\} = \{\boldsymbol{\eta}_1^{[m_1]}, \boldsymbol{\eta}_2^{[m_2]}, \boldsymbol{\eta}_3^{[m_3]}\}$, where $n = m_1 + m_2 + m_3 - 1$ and $\boldsymbol{\eta}^{[m]}$ means that the point $\boldsymbol{\eta}$ is repeated m times. More precisely,

$$M_{\Xi}(\boldsymbol{x}) = \frac{n(n-1)}{2A(\langle \Xi \rangle)} B^{n-2}_{m_1-1, m_2-1, m_3-1}(\boldsymbol{x}), \quad \boldsymbol{x} \in \langle \{\boldsymbol{\eta}_1, \boldsymbol{\eta}_2, \boldsymbol{\eta}_3\} \rangle,$$

where $B^d_{j_1, j_2, j_3}$ is a Bernstein polynomial of degree d defined by

$$B^d_{j_1, j_2, j_3}(\boldsymbol{x}) := \frac{d!}{j_1! j_2! j_3!} \beta_1^{j_1} \beta_2^{j_2} \beta_3^{j_3}, \quad \boldsymbol{x} \in \langle \{\boldsymbol{\eta}_1, \boldsymbol{\eta}_2, \boldsymbol{\eta}_3\} \rangle,$$

and $(\beta_1, \beta_2, \beta_3) \in \mathbb{R}^3$ are the barycentric coordinates of $\boldsymbol{x}$ given by

$$\boldsymbol{x} = \beta_1 \boldsymbol{\eta}_1 + \beta_2 \boldsymbol{\eta}_2 + \beta_3 \boldsymbol{\eta}_3, \quad \beta_1 + \beta_2 + \beta_3 = 1.$$

2.2. Simplex-splines on the Clough–Tocher split

Let us focus on the triangle $\mathcal{T} := \langle \{\boldsymbol{p}_1, \boldsymbol{p}_2, \boldsymbol{p}_3\} \rangle$ in $\mathbb{R}^2$. Using the barycenter $\boldsymbol{p}_{\mathcal{T}} := (\boldsymbol{p}_1 + \boldsymbol{p}_2 + \boldsymbol{p}_3)/3$, we can split $\mathcal{T}$ into three subtriangles: $\mathcal{T}_1 := \langle \{\boldsymbol{p}_{\mathcal{T}}, \boldsymbol{p}_2, \boldsymbol{p}_3\} \rangle$, $\mathcal{T}_2 := \langle \{\boldsymbol{p}_1, \boldsymbol{p}_{\mathcal{T}}, \boldsymbol{p}_3\} \rangle$, and $\mathcal{T}_3 := \langle \{\boldsymbol{p}_1, \boldsymbol{p}_2, \boldsymbol{p}_{\mathcal{T}}\} \rangle$. This is called the Clough–Tocher split of $\mathcal{T}$ and is denoted by $\mathcal{T}_{\mathrm{CT}}$; see Fig. 1 for an illustration.

Let $\mathbb{S}^1_d(\mathcal{T}_{\mathrm{CT}})$ be the C^1 spline space of degree $d \geq 3$ on $\mathcal{T}_{\mathrm{CT}}$, i.e.,

$$\mathbb{S}^1_d(\mathcal{T}_{\mathrm{CT}}) := \{s \in C^1(\mathcal{T}) : s|_{\mathcal{T}_j} \in \mathbb{P}_d,\ j = 1, 2, 3\},$$

where $\mathbb{P}_d$ is the space of bivariate polynomials of total degree $\leq d$. From [26,29] we know that

$$\dim(\mathbb{S}^1_d(\mathcal{T}_{\mathrm{CT}})) = \binom{d+2}{2} + 2\binom{d-1}{2} = \frac{3}{2}(d^2 - d + 2). \tag{1}$$

Remark 1. Any spline $s \in \mathbb{S}^1_d(\mathcal{T}_{\mathrm{CT}})$ can be identified by means of the following Hermite data:

1. the value and gradient (i.e., D_x and D_y) at each point $\boldsymbol{p}_j$, $j = 1, 2, 3$;
2. the value at $d-3$ distinct points in the interior of each edge $\mathcal{E}_j := \langle \{\boldsymbol{p}_1, \boldsymbol{p}_2, \boldsymbol{p}_3\} \setminus \{\boldsymbol{p}_j\} \rangle$, $j = 1, 2, 3$;
3. the normal derivative at $d-2$ distinct points in the interior of each edge $\mathcal{E}_j := \langle \{\boldsymbol{p}_1, \boldsymbol{p}_2, \boldsymbol{p}_3\} \setminus \{\boldsymbol{p}_j\} \rangle$, $j = 1, 2, 3$;

and if $d \geq 4$,

4. the value and gradient at the barycenter $\boldsymbol{p}_{\mathcal{T}}$;
5. the value at $d-4$ distinct points in the interior of each edge $\mathcal{E}_{j,\mathcal{T}} := \langle \boldsymbol{p}_j, \boldsymbol{p}_{\mathcal{T}} \rangle$, $j = 1, 2, 3$;
6. the normal derivative at $d-4$ distinct points in the interior of each edge $\mathcal{E}_{j,\mathcal{T}} := \langle \boldsymbol{p}_j, \boldsymbol{p}_{\mathcal{T}} \rangle$, $j = 1, 2, 3$;

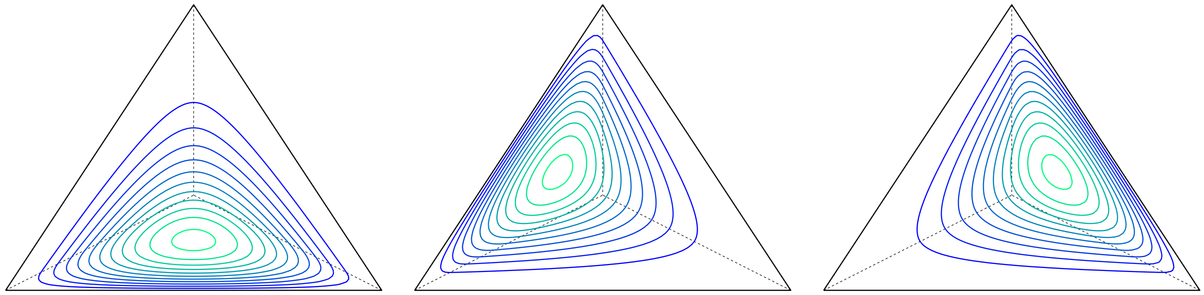

(a) $S^3[2,2,1;1]$ (b) $S^3[2,1,2;1]$ (c) $S^3[1,2,2;1]$

Fig. 2. The normalized simplex-splines in $\mathcal{S}^d$ indexed by $\mathcal{I}_1^d$ for $d = 3$.

7. the value at $\frac{1}{2}(d-4)(d-5)$ distinct points in the interior of each subtriangle $\mathcal{T}_j$ chosen such that if a polynomial of degree $d-6$ vanishes at those points, then it is identically zero.

The above Hermite data can be used to define a nodal finite element basis on the Clough–Tocher split; see [26] and also Remark 5. In this paper, we focus on an alternative basis of normalized simplex-splines, developed in [23].

Let i_1, i_2, i_3 and ℓ be nonnegative integers such that $i_1 + i_2 + i_3 + \ell = d + 3$. We introduce the notation $\triangle[i_1, i_2, i_3; \ell] := M_\Xi$, where $\Xi = \{\boldsymbol{p}_1^{[i_1]}, \boldsymbol{p}_2^{[i_2]}, \boldsymbol{p}_3^{[i_3]}, \boldsymbol{p}_{\mathcal{T}}^{[\ell]}\}$. Recall that $\boldsymbol{p}^{[m]}$ means that the point $\boldsymbol{p}$ is repeated m times (so it has multiplicity m). Then, we define the following two types of indices, to distinguish between two types of simplex-splines of degree d:

- **Type 0:** $\mathcal{I}_0^d$ is the set of indices $(i_1, i_2, i_3; 0)$ for all $i_1 \geq 1$, $i_2 \geq 1$, $i_3 \geq 1$, with $i_1 + i_2 + i_3 = d + 3$ and there is at least one j such that $i_j = 1$.
- **Type 1:** $\mathcal{I}_1^d$ is the set of indices $(i_1, i_2, i_3; \ell)$ for all $i_1 \geq 1$, $i_2 \geq 1$, $i_3 \geq 1$, $\ell \geq 1$, with $i_1 + i_2 + i_3 + \ell = d + 3$ and there is exactly one j such that $i_j = 1$ (and so $i_k \geq 2$ for all $k \neq j$).

The simplex-spline $\triangle[i_1, i_2, i_3; \ell]$ is said to be of Type 0 if $(i_1, i_2, i_3; \ell) \in \mathcal{I}_0^d$, while it is of Type 1 if $(i_1, i_2, i_3; \ell) \in \mathcal{I}_1^d$. Finally, $\mathcal{I}^d := \mathcal{I}_0^d \cup \mathcal{I}_1^d$. Note that $\#\mathcal{I}_0^d = 3d$ and $\#\mathcal{I}_1^d = 3(d-1)(d-2)/2$, which implies that $\#\mathcal{I}^d = \dim(\mathbb{S}_d^1(\mathcal{T}_{\mathrm{CT}}))$.

This allows us to construct a normalized simplex-spline basis for the space $\mathbb{S}_d^1(\mathcal{T}_{\mathrm{CT}})$ as follows [23]. We define the set $\mathcal{S}^d := \{S^d[i_1, i_2, i_3; \ell] \in C^1(\mathcal{T}) : (i_1, i_2, i_3; \ell) \in \mathcal{I}^d\}$, where

$$S^d[i_1, i_2, i_3; \ell] := \frac{2A(\mathcal{T})}{(d+1)(d+2)} \begin{cases} \triangle[i_1, i_2, i_3; 0], & (i_1, i_2, i_3; 0) \in \mathcal{I}_0^d, \\ \frac{1}{3}\triangle[i_1, i_2, i_3; \ell], & (i_1, i_2, i_3; \ell) \in \mathcal{I}_1^d. \end{cases} \tag{2}$$

It has been shown in [23] that the functions in $\mathcal{S}^d$ are nonnegative and form a partition of unity on $\mathcal{T}$. Moreover, they form a basis for the space $\mathbb{S}_d^1(\mathcal{T}_{\mathrm{CT}})$. From the properties described in Section 2.1 and $d = n - 2$, it is easily seen that the functions in $\mathcal{S}^d$ indexed by $\mathcal{I}_0^d$ are nothing but Bernstein polynomials on $\mathcal{T}$, namely

$$S^d[i_1, i_2, i_3; 0] = B^d_{i_1-1, i_2-1, i_3-1}, \quad (i_1, i_2, i_3; 0) \in \mathcal{I}_0^d. \tag{3}$$

Example 2. Suppose $d = 3$. In view of (1), the dimension of $\mathbb{S}_3^1(\mathcal{T}_{\mathrm{CT}})$ is 12. The functions in $\mathcal{S}^3$ indexed by $\mathcal{I}_0^3$ are given by

$$\begin{aligned} &S^3[4,1,1;0] = B^3_{3,0,0}, \quad S^3[3,2,1;0] = B^3_{2,1,0}, \quad S^3[2,3,1;0] = B^3_{1,2,0}, \\ &S^3[1,4,1;0] = B^3_{0,3,0}, \quad S^3[1,3,2;0] = B^3_{0,2,1}, \quad S^3[1,2,3;0] = B^3_{0,1,2}, \\ &S^3[1,1,4;0] = B^3_{0,0,3}, \quad S^3[2,1,3;0] = B^3_{1,0,2}, \quad S^3[3,1,2;0] = B^3_{2,0,1}. \end{aligned}$$

The functions in $\mathcal{S}^3$ indexed by $\mathcal{I}_1^3$ are given by

$$S^3[2,2,1;1], \quad S^3[2,1,2;1], \quad S^3[1,2,2;1].$$

These functions are visualized in Fig. 2. With simple computations, we obtain

$$\begin{aligned} &S^3[2,2,1;1]|_{\mathcal{T}_1} = (B^3_{2,1,0} - B^3_{3,0,0})|_{\mathcal{T}_1}, \\ &S^3[2,2,1;1]|_{\mathcal{T}_2} = (B^3_{1,2,0} - B^3_{0,3,0})|_{\mathcal{T}_2}, \\ &S^3[2,2,1;1]|_{\mathcal{T}_3} = (B^3_{1,1,1} - B^3_{1,0,2} - B^3_{0,1,2} + 2B^3_{0,0,3})|_{\mathcal{T}_3}. \end{aligned}$$

By exploiting symmetry, similar expressions are obtained for $S^3[2,1,2;1]$ and $S^3[1,2,2;1]$. Note that $S^3[2,2,1;1] + S^3[2,1,2;1] + S^3[1,2,2;1] = B^3_{1,1,1}$. All Bernstein polynomials used in this example are defined on $\mathcal{T}$.

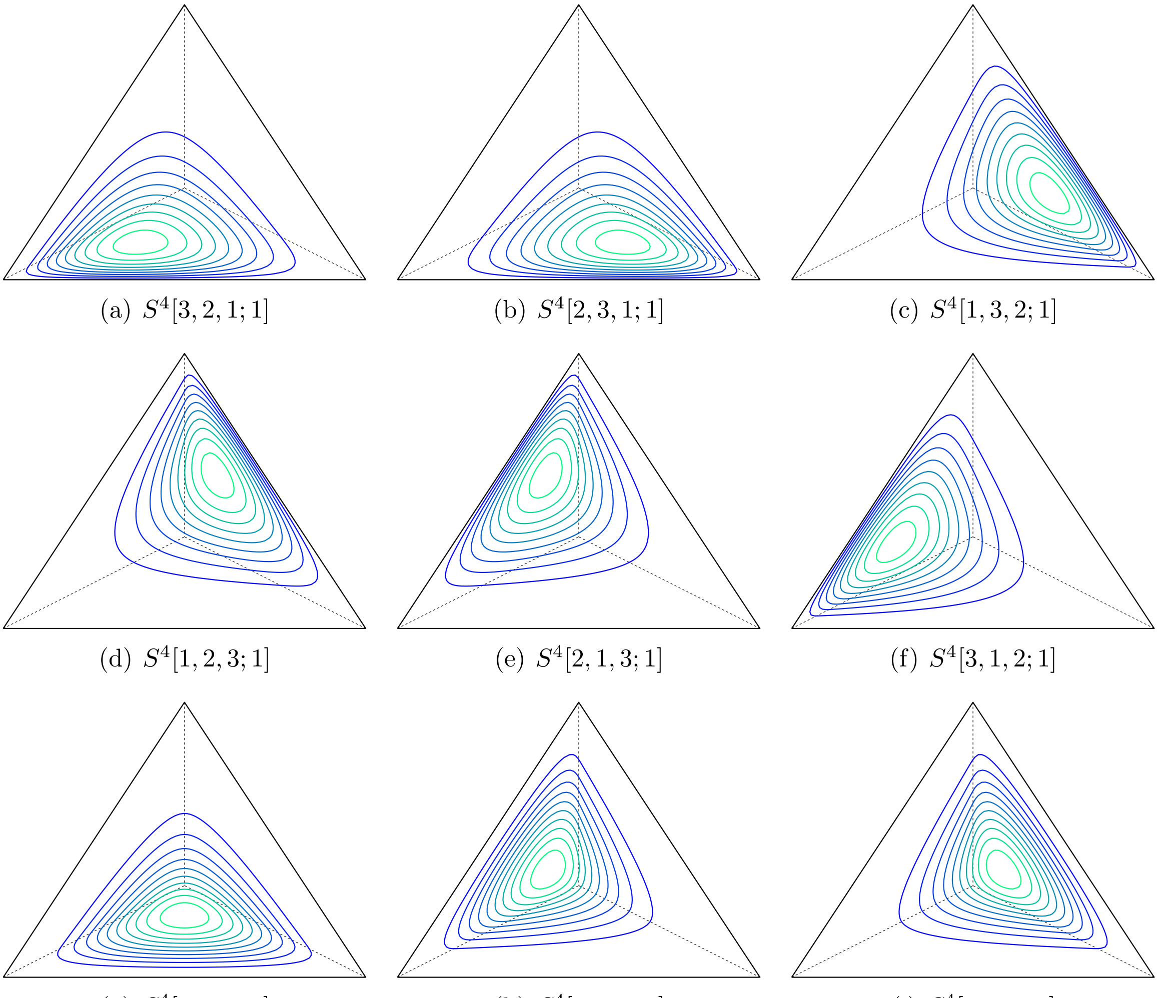

(a) $S^4[3,2,1;1]$ (b) $S^4[2,3,1;1]$ (c) $S^4[1,3,2;1]$
(d) $S^4[1,2,3;1]$ (e) $S^4[2,1,3;1]$ (f) $S^4[3,1,2;1]$
(g) $S^4[2,2,1;2]$ (h) $S^4[2,1,2;2]$ (i) $S^4[1,2,2;2]$

Fig. 3. The normalized simplex-splines in $\mathcal{S}^d$ indexed by $\mathcal{I}_1^d$ for $d = 4$.

Example 3. Suppose $d = 4$. In view of (1), the dimension of $\mathbb{S}_4^1(\mathcal{T}_{\mathrm{CT}})$ is 21. The functions in $\mathcal{S}^4$ indexed by $\mathcal{I}_0^4$ are given by

$$
\begin{aligned}
&S^4[5,1,1;0] = B^4_{4,0,0}, \quad S^4[4,2,1;0] = B^4_{3,1,0}, \quad S^4[3,3,1;0] = B^4_{2,2,0},\\
&S^4[2,4,1;0] = B^4_{1,3,0}, \quad S^4[1,5,1;0] = B^4_{0,4,0}, \quad S^4[1,4,2;0] = B^4_{0,3,1},\\
&S^4[1,3,3;0] = B^4_{0,2,2}, \quad S^4[1,2,4;0] = B^4_{0,1,3}, \quad S^4[1,1,5;0] = B^4_{0,0,4},\\
&S^4[2,1,4;0] = B^4_{1,0,3}, \quad S^4[3,1,3;0] = B^4_{2,0,2}, \quad S^4[4,1,2;0] = B^4_{3,0,1}.
\end{aligned}
$$

The functions in $\mathcal{S}^4$ indexed by $\mathcal{I}_1^4$ are given by

$$
\begin{aligned}
&S^4[3,2,1;1], \quad S^4[2,3,1;1], \quad S^4[1,3,2;1],\\
&S^4[1,2,3;1], \quad S^4[2,1,3;1], \quad S^4[3,1,2;1],\\
&S^4[2,2,1;2], \quad S^4[2,1,2;2], \quad S^4[1,2,2;2].
\end{aligned}
$$

These functions are visualized in Fig. 3. With simple computations, we obtain

$$
\begin{aligned}
&S^4[3,2,1;1]|_{\mathcal{T}_1} = (B^4_{3,1,0} - B^4_{4,0,0})|_{\mathcal{T}_1},\\
&S^4[3,2,1;1]|_{\mathcal{T}_2} = (B^4_{2,2,0} - B^4_{1,3,0} + B^4_{0,4,0})|_{\mathcal{T}_2},\\
&S^4[3,2,1;1]|_{\mathcal{T}_3} = (B^4_{2,1,1} - B^4_{2,0,2} - B^4_{1,1,2} + 2B^4_{1,0,3} + B^4_{0,1,3} - 3B^4_{0,0,4})|_{\mathcal{T}_3},
\end{aligned}
$$

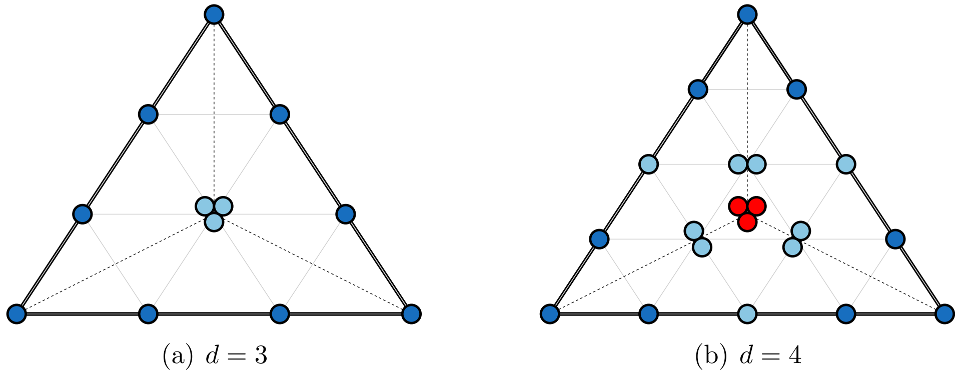

Fig. 4. The domain points $\boldsymbol{d}^d(i_1, i_2, i_3; \ell)$ of the normalized simplex-splines $\mathcal{S}^d[i_1, i_2, i_3; \ell]$, $(i_1, i_2, i_3; \ell) \in \mathcal{I}^d$, for the cases $d = 3$ and $d = 4$. Coinciding domain points are slightly perturbed to visualize them properly. The vertex domain points are colored in blue, the edge domain points in cyan, and the triangle domain points in red. (For interpretation of the colors in this figure, the reader is referred to the web version of this article.)

and

$$
\begin{aligned}
\mathcal{S}^4[2,2,1;2]|_{\mathcal{T}_1} &= 3(B^4_{3,1,0} - 2B^4_{4,0,0})|_{\mathcal{T}_1},\\
\mathcal{S}^4[2,2,1;2]|_{\mathcal{T}_2} &= 3(B^4_{1,3,0} - 2B^4_{0,4,0})|_{\mathcal{T}_2},\\
\mathcal{S}^4[2,2,1;2]|_{\mathcal{T}_3} &= 3(B^4_{1,1,2} - 2B^4_{1,0,3} - 2B^4_{0,1,3} + 6B^4_{0,0,4})|_{\mathcal{T}_3}.
\end{aligned}
$$

By exploiting symmetry, similar expressions are obtained for the other functions in $\mathcal{S}^4$ of Type 1. All Bernstein polynomials used in this example are defined on $\mathcal{T}$.

Any spline of the space $s \in \mathbb{S}^1_d(\mathcal{T}_{\mathrm{CT}})$ can be uniquely described in terms of the basis $\mathcal{S}^d$, i.e.,

$$
s(\boldsymbol{x}) = \sum_{(i_1,i_2,i_3;\ell)\in\mathcal{I}^d} c(i_1, i_2, i_3; \ell)\, \mathcal{S}^d[i_1, i_2, i_3; \ell](\boldsymbol{x}), \quad \boldsymbol{x} \in \mathcal{T},
$$

for some values $c(i_1, i_2, i_3; \ell) \in \mathbb{R}$. From [23] we know that

$$
\boldsymbol{x} = \sum_{(i_1,i_2,i_3;\ell)\in\mathcal{I}^d} \boldsymbol{d}^d(i_1, i_2, i_3; \ell)\, \mathcal{S}^d[i_1, i_2, i_3; \ell](\boldsymbol{x}), \quad \boldsymbol{x} \in \mathcal{T},
$$

where

$$
\boldsymbol{d}^d(i_1, i_2, i_3; 0) := \sum_{k=1}^{3} \frac{i_k - 1}{d} \boldsymbol{p}_k, \quad (i_1, i_2, i_3; 0) \in \mathcal{I}^d_0,
$$

and

$$
\boldsymbol{d}^d(i_1, i_2, i_3; \ell) := \sum_{k=1}^{3} \frac{i_k - 1}{d} \boldsymbol{p}_k + \frac{1}{d}\boldsymbol{p}_j + \frac{\ell - 1}{d}\boldsymbol{p}_{\mathcal{T}}, \quad (i_1, i_2, i_3; \ell) \in \mathcal{I}^d_1,\ i_j = 1.
$$

The points $\boldsymbol{d}^d(i_1, i_2, i_3; \ell) \in \mathbb{R}^2$ are called the domain points of the normalized simplex-splines $\mathcal{S}^d[i_1, i_2, i_3; \ell]$, $(i_1, i_2, i_3; \ell) \in \mathcal{I}^d$. It is easy to see that all these points belong to $\mathcal{T}$. In particular, the domain points related to $\mathcal{I}^d_0$ are all on the boundary of $\mathcal{T}$. In view of (3), the latter points are domain points of standard Bernstein polynomials of degree d. With the aim of constructing C^1 splines on triangulations (see Section 3), we classify the domain points into the following three groups:

- **Vertex domain points:** The points $\{\boldsymbol{d}^d(i_1, i_2, i_3; 0) : (i_1, i_2, i_3; 0) \in \mathcal{I}^d_0,\ i_j \geq d\}$ are the domain points associated with $\boldsymbol{p}_j$, $j = 1, 2, 3$.
- **Edge domain points:** The points $\{\boldsymbol{d}^d(i_1, i_2, i_3; \ell) : (i_1, i_2, i_3; \ell) \in \mathcal{I}^d,\ i_1 < d,\ i_2 < d,\ i_3 < d,\ i_j = 1,\ \ell \leq 1\}$ are the domain points associated with the edge $\mathcal{E}_j := \langle \{\boldsymbol{p}_1, \boldsymbol{p}_2, \boldsymbol{p}_3\} \setminus \{\boldsymbol{p}_j\} \rangle$, $j = 1, 2, 3$.
- **Triangle domain points:** The points $\{\boldsymbol{d}^d(i_1, i_2, i_3; \ell) : (i_1, i_2, i_3; \ell) \in \mathcal{I}^d_1,\ \ell \geq 2\}$ are the domain points associated with the triangle $\mathcal{T}$.

For the cases $d = 3$ and $d = 4$, the domain points are depicted in Fig. 4. Note that domain points related to $\mathcal{I}^d_1$ may coincide. Such points have been slightly perturbed in the figure to visualize them properly. The three groups of domain points are indicated with a different color.

Remark 4. Instead of representing a spline $s \in \mathbb{S}^1_d(\mathcal{T}_{\mathrm{CT}})$ in terms of the simplex-spline basis $\mathcal{S}^d$, one could alternatively consider three separate representations in terms of the Bernstein polynomial basis on the subtriangles $\mathcal{T}_j$, $j = 1, 2, 3$, as proposed in [30]. However, the latter approach involves

$$3\dim(\mathbb{P}_d) = 3\binom{d+2}{2} = \frac{3}{2}(d^2+3d+2)$$

parameters. Thus, compared with (1), it requires $6d$ more parameters than working with a basis as $\mathcal{S}^d$.

Remark 5. The Hermite data described in Remark 1 could also be utilized to define a basis for the space $\mathbb{S}^1_d(\mathcal{T}_{\mathrm{CT}})$, a so-called nodal finite element basis [26]. More precisely, since each spline $s \in \mathbb{S}^1_d(\mathcal{T}_{\mathrm{CT}})$ is identified by such a set of Hermite data, a basis function can be obtained by taking one of these parameters equal to 1 and all the others equal to 0. Note that this basis does not form a partition of unity. Moreover, it is known that a B-spline-like basis is computationally more stable than a nodal basis using derivative information (also called a Hermite basis). We refer the reader to the numerical experimentation (Table 1) in [18] for an example. Therefore, $\mathcal{S}^d$ seems to be a more appealing basis for $\mathbb{S}^1_d(\mathcal{T}_{\mathrm{CT}})$ in practice.

3. C^1 splines on triangulations

In this section, we discuss the C^1 connection between adjacent triangles and how to deal with a general triangulation.

Given a triangulation $\triangle$ of a domain Ω, let $\triangle_{\mathrm{CT}}$ be the corresponding refinement obtained by taking the Clough–Tocher split of each triangle $\mathcal{T}$ of $\triangle$ as defined in the previous section. Then, we consider the C^1 spline space of degree $d \geq 3$ on $\triangle_{\mathrm{CT}}$, i.e.,

$$\mathbb{S}^1_d(\triangle_{\mathrm{CT}}) := \{s \in C^1(\Omega) : s|_{\mathcal{T}} \in \mathbb{S}^1_d(\mathcal{T}_{\mathrm{CT}}),\ \mathcal{T} \in \triangle\}.$$

The dimension of $\mathbb{S}^1_d(\triangle_{\mathrm{CT}})$ can be established by following standard techniques for analysis of spline spaces over triangulations. Using the theory from [13], one deduces that

$$\dim(\mathbb{S}^1_d(\triangle_{\mathrm{CT}})) = 3N_v + (2d-5)N_e + \frac{3}{2}(d-2)(d-3)N_t, \tag{4}$$

where N_v, N_e, N_t are the number of vertices, edges, triangles of the triangulation, respectively. When $\triangle$ consists of a single triangle ($N_v = 3$, $N_e = 3$, $N_t = 1$), we exactly recover the dimension formula in (1). For the cases $d = 3, 4$, the formula in (4) simplifies to

$$\dim(\mathbb{S}^1_3(\triangle_{\mathrm{CT}})) = 3N_v + N_e, \quad \dim(\mathbb{S}^1_4(\triangle_{\mathrm{CT}})) = 3(N_v + N_e + N_t).$$

To obtain a representation for splines in $\mathbb{S}^1_d(\triangle_{\mathrm{CT}})$, we use the local basis described in the previous section for each triangle of $\triangle$. This gives $N_{\mathcal{T}} := 3(d^2-d+2)/2$ normalized simplex-splines multiplied by N_t. Then, we impose C^1 smoothness conditions across the edges of $\triangle$, which allows for an easy elimination of parameters till the correct number of degrees of freedom of the space.

Let us first look at conditions that ensure C^0 and C^1 smoothness across a common edge between two triangles. These conditions have been provided in [23]. Suppose

$$s = \sum_{(i_1,i_2,i_3;\ell)\in\mathcal{I}^d} c^d(i_1,i_2,i_3;\ell)\, S^d[i_1,i_2,i_3;\ell], \quad \tilde{s} = \sum_{(i_1,i_2,i_3;\ell)\in\mathcal{I}^d} \tilde{c}^d(i_1,i_2,i_3;\ell)\, \tilde{S}^d[i_1,i_2,i_3;\ell] \tag{5}$$

are two splines of degree d defined on the triangles $\mathcal{T} := \langle\{\boldsymbol{p}_1,\boldsymbol{p}_2,\boldsymbol{p}_3\}\rangle$ and $\tilde{\mathcal{T}} := \langle\{\boldsymbol{p}_1,\boldsymbol{p}_2,\tilde{\boldsymbol{p}}_3\}\rangle$, respectively, sharing the edge $\mathcal{E}_3 := \langle\{\boldsymbol{p}_1,\boldsymbol{p}_2\}\rangle$. Then, s and $\tilde{s}$ join together with C^r smoothness ($r = 0, 1$) across the edge $\mathcal{E}_3$ if and only if

- $r = 0$: for all $(i_1, i_2, 1; 0) \in \mathcal{I}^d_0$ we have

$$\tilde{c}^d(i_1,i_2,1;0) = c^d(i_1,i_2,1;0); \tag{6}$$

- $r = 1$: in addition to $r = 0$, for all $(i_1, i_2, 2; 0) \in \mathcal{I}^d_0$ we have

$$\tilde{c}^d(i_1,i_2,2;0) = \gamma_1\, c^d(i_1+1,i_2,1;0) + \gamma_2\, c^d(i_1,i_2+1,1;0) + \gamma_3\, c^d(i_1,i_2,2;0), \tag{7}$$

  and for all $(i_1, i_2, 1; 1) \in \mathcal{I}^d_1$ we have

$$\tilde{c}^d(i_1,i_2,1;1) = \gamma_1\, c^d(i_1+1,i_2,1;0) + \gamma_2\, c^d(i_1,i_2+1,1;0) + \gamma_3\, c^d(i_1,i_2,1;1), \tag{8}$$

  where $\tilde{\boldsymbol{p}}_3 = \gamma_1\boldsymbol{p}_1 + \gamma_2\boldsymbol{p}_2 + \gamma_3\boldsymbol{p}_3$, $\gamma_1 + \gamma_2 + \gamma_3 = 1$.

These smoothness conditions exhibit a large similarity to the smoothness conditions between two polynomials represented in the Bernstein basis on two adjacent triangles; see [13].

Example 6. Suppose $d = 3$. The conditions for C^0 smoothness across the edge $\mathcal{E}_3$ are given by

$$\tilde{c}^3(4,1,1;0) = c^3(4,1,1;0), \quad \tilde{c}^3(3,2,1;0) = c^3(3,2,1;0),$$
$$\tilde{c}^3(2,3,1;0) = c^3(2,3,1;0), \quad \tilde{c}^3(1,4,1;0) = c^3(1,4,1;0).$$

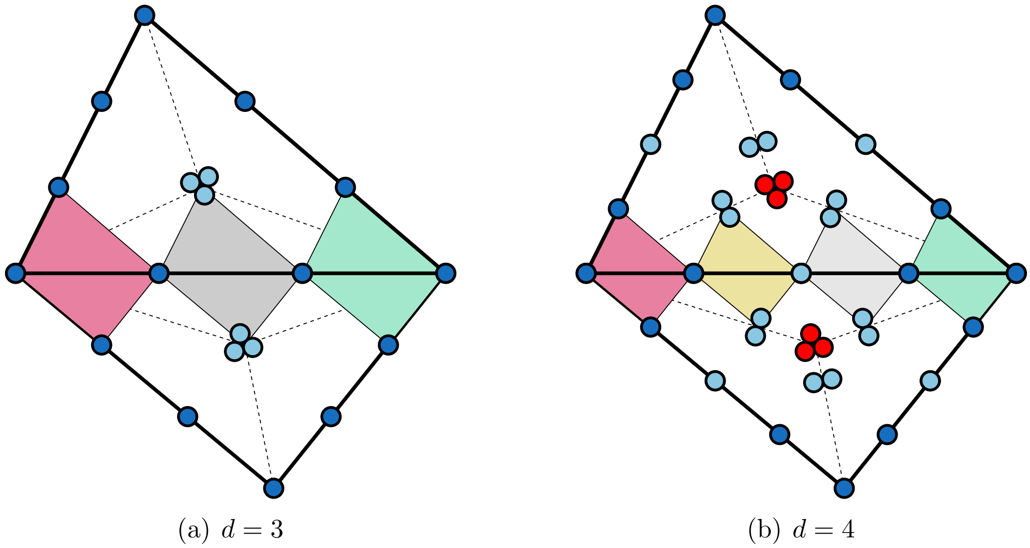

Fig. 5. Visualization of the geometric requirement to obtain C^1 smoothness across the common edge between two adjacent triangles, for the cases $d = 3$ and $d = 4$. Each set of four domain points forming the corners of a colored quadrilateral area requires that the four corresponding control points must be coplanar. The same color code is used for the domain points as in Fig. 4.

In addition to the above ones, the conditions for C^1 smoothness across the edge $\mathcal{E}_3$ are given by

$$\tilde{c}^3(3,1,2;0) = \gamma_1\, c^3(4,1,1;0) + \gamma_2\, c^3(3,2,1;0) + \gamma_3\, c^3(3,1,2;0),$$
$$\tilde{c}^3(2,2,1;1) = \gamma_1\, c^3(3,2,1;0) + \gamma_2\, c^3(2,3,1;0) + \gamma_3\, c^3(2,2,1;1),$$
$$\tilde{c}^3(1,3,2;0) = \gamma_1\, c^3(2,3,1;0) + \gamma_2\, c^3(1,4,1;0) + \gamma_3\, c^3(1,3,2;0).$$

Example 7. Suppose $d = 4$. The conditions for C^0 smoothness across the edge $\mathcal{E}_3$ are given by

$$\tilde{c}^4(5,1,1;0) = c^4(5,1,1;0), \quad \tilde{c}^4(4,2,1;0) = c^4(4,2,1;0),$$
$$\tilde{c}^4(3,3,1;0) = c^4(3,3,1;0), \quad \tilde{c}^4(2,4,1;0) = c^4(2,4,1;0),$$
$$\tilde{c}^4(1,5,1;0) = c^4(1,5,1;0).$$

In addition to the above ones, the conditions for C^1 smoothness across the edge $\mathcal{E}_3$ are given by

$$\tilde{c}^4(4,1,2;0) = \gamma_1\, c^4(5,1,1;0) + \gamma_2\, c^4(4,2,1;0) + \gamma_3\, c^4(4,1,2;0),$$
$$\tilde{c}^4(3,2,1;1) = \gamma_1\, c^4(4,2,1;0) + \gamma_2\, c^4(3,3,1;0) + \gamma_3\, c^4(3,2,1;1),$$
$$\tilde{c}^4(2,3,1;1) = \gamma_1\, c^4(3,3,1;0) + \gamma_2\, c^4(2,4,1;0) + \gamma_3\, c^4(2,3,1;1),$$
$$\tilde{c}^4(1,4,2;0) = \gamma_1\, c^4(2,4,1;0) + \gamma_2\, c^4(1,5,1;0) + \gamma_3\, c^4(1,4,2;0).$$

By associating the coefficients $c^d(i_1,i_2,i_3;\ell)$ of s in (5) with the corresponding domain points $\boldsymbol{d}^d(i_1,i_2,i_3;\ell)$ on $\mathcal{T}$, we obtain the control points of s, denoted by $\boldsymbol{c}^d(i_1,i_2,i_3;\ell) := \big(\boldsymbol{d}^d(i_1,i_2,i_3;\ell), c^d(i_1,i_2,i_3;\ell)\big)$, for all $(i_1,i_2,i_3;\ell) \in \mathcal{I}^d$. Similarly, the control points of $\tilde{s}$ are defined as $\tilde{\boldsymbol{c}}^d(i_1,i_2,i_3;\ell) := \big(\tilde{\boldsymbol{d}}^d(i_1,i_2,i_3;\ell), \tilde{c}^d(i_1,i_2,i_3;\ell)\big)$, for all $(i_1,i_2,i_3;\ell) \in \mathcal{I}^d$. With the aid of the control points, we can give a geometric interpretation to the C^1 smoothness conditions (6)–(8) described above. More precisely, these conditions are geometrically equivalent to requiring that d pairs of triplets of control points, defined on $\mathcal{T}$ and $\tilde{\mathcal{T}}$, are coplanar, namely

- $\big(\boldsymbol{c}^d(d+1,1,1;0),\ \boldsymbol{c}^d(d,2,1;0),\ \boldsymbol{c}^d(d,1,2;0)\big)$ and $\big(\tilde{\boldsymbol{c}}^d(d+1,1,1;0),\ \tilde{\boldsymbol{c}}^d(d,2,1;0),\ \tilde{\boldsymbol{c}}^d(d,1,2;0)\big)$ are coplanar;
- $\big(\boldsymbol{c}^d(d-i+2,i,1;0),\ \boldsymbol{c}^d(d-i+1,i+1,1;0),\ \boldsymbol{c}^d(d-i+1,i,1;1)\big)$ and $\big(\tilde{\boldsymbol{c}}^d(d-i+2,i,1;0),\ \tilde{\boldsymbol{c}}^d(d-i+1,i+1,1;0),\ \tilde{\boldsymbol{c}}^d(d-i+1,i,1;1)\big)$ are coplanar, for all $i = 2,\dots,d-1$;
- $\big(\boldsymbol{c}^d(2,d,1;0),\ \boldsymbol{c}^d(1,d+1,1;0),\ \boldsymbol{c}^d(1,d,2;0)\big)$ and $\big(\tilde{\boldsymbol{c}}^d(2,d,1;0),\ \tilde{\boldsymbol{c}}^d(1,d+1,1;0),\ \tilde{\boldsymbol{c}}^d(1,d,2;0)\big)$ are coplanar.

Fig. 5 illustrates an example of the geometric requirement to obtain C^1 smoothness on two adjacent triangles, for $d = 3$ and $d = 4$.

With the aim of constructing a stable global basis for the spline space $\mathbb{S}^1_d(\triangle_{\mathrm{CT}})$, we make use of the concept of minimal determining sets. Minimal determining sets are a common tool in the context of Bernstein polynomials [13], but have recently also been applied

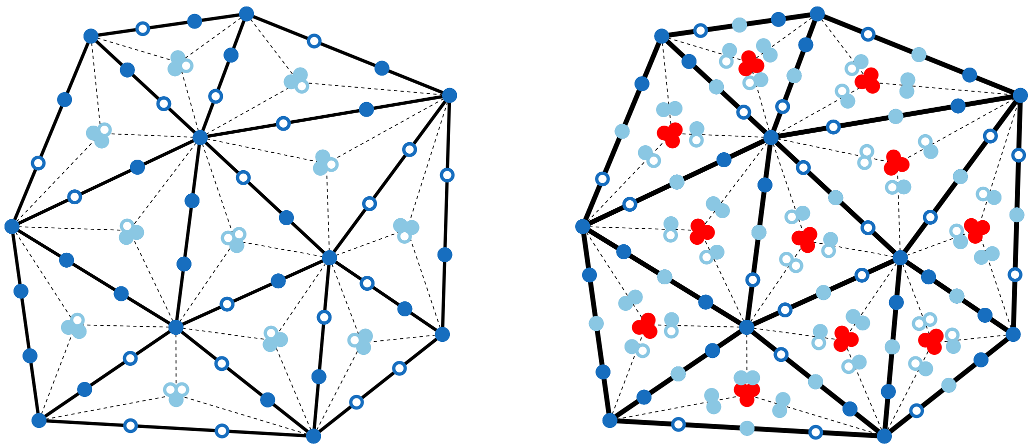

(a) $d = 3$ (b) $d = 4$

Fig. 6. A minimal determining set for $\mathbb{S}^1_d(\triangle_{\mathrm{CT}})$, consisting of the domain points indicated with filled bullets, for the cases $d = 3$ and $d = 4$. The coefficients related to these domain points are free to choose, while the others are determined by imposing the C^1 smoothness conditions. The domain points associated with a vertex are colored in blue (filled and empty bullets), the domain points associated with an edge in cyan (filled and empty bullets), and the domain points associated with a triangle in red (filled bullets). The same color code is used for the domain points as in Fig. 4.

to simplex-splines [21,31]. Hereafter, for each triangle $\mathcal{T} \in \triangle$, we denote the normalized simplex-splines in (2) related to $\mathcal{T}$ by $S^d_{k,\mathcal{T}}$, $k = 1, \dots, N_{\mathcal{T}}$. The restriction of a spline $s \in \mathbb{S}^1_d(\triangle_{\mathrm{CT}})$ onto a triangle $\mathcal{T} \in \triangle$ can then be expressed as

$$s|_{\mathcal{T}} = \sum_{k=1}^{N_{\mathcal{T}}} c^d_{k,\mathcal{T}}\, S^d_{k,\mathcal{T}}. \tag{9}$$

Similarly, we denote the corresponding domain points by $\boldsymbol{d}^d_{k,\mathcal{T}}$, $k = 1, \dots, N_{\mathcal{T}}$, and we define the multisets

$$\mathcal{D}^d_{\mathcal{T}} := \{\boldsymbol{d}^d_{k,\mathcal{T}} : k = 1, \dots, N_{\mathcal{T}}\}, \quad \mathcal{D}^d_{\triangle} := \bigcup_{\mathcal{T} \in \triangle} \mathcal{D}^d_{\mathcal{T}}.$$

Recall that the domain points in $\mathcal{D}^d_{\mathcal{T}}$ can be coinciding (see also Fig. 4). Now, we build the multiset $\mathcal{M}^d_{\triangle} \subseteq \mathcal{D}^d_{\triangle}$ consisting of the following domain points:

- For each vertex $\boldsymbol{p}$ of $\triangle$, choose a triangle $\mathcal{T} \in \triangle$ that has $\boldsymbol{p}$ as a vertex, and select the three vertex domain points in $\mathcal{D}^d_{\mathcal{T}}$ associated with $\boldsymbol{p}$.
- For each edge $\mathcal{E}$ of $\triangle$, choose a triangle $\mathcal{T} \in \triangle$ containing this edge and select the edge domain points in $\mathcal{D}^d_{\mathcal{T}}$ associated with $\mathcal{E}$.
- For each triangle $\mathcal{T}$ of $\triangle$, select the triangle domain points in $\mathcal{D}^d_{\mathcal{T}}$ associated with $\mathcal{T}$.

The multiset $\mathcal{M}^d_{\triangle}$ is a so-called Minimal Determining Set (MDS) for $\mathbb{S}^1_d(\triangle_{\mathrm{CT}})$. That means that the cardinality of $\mathcal{M}^d_{\triangle}$ is equal to $\dim(\mathbb{S}^1_d(\triangle_{\mathrm{CT}}))$; see (4). Moreover, if $s \in \mathbb{S}^1_d(\triangle_{\mathrm{CT}})$ is locally represented as in (9) on all $\mathcal{T} \in \triangle$ and s has all the coefficients associated with domain points in $\mathcal{M}^d_{\triangle}$ equal to zero, then $s \equiv 0$ (this follows from the C^1 smoothness conditions). An example of a minimal determining set is depicted in Fig. 6 for $d = 3$ and $d = 4$.

We are now ready to construct a global basis for $\mathbb{S}^1_d(\triangle_{\mathrm{CT}})$. Given a minimal determining set $\mathcal{M}^d_{\triangle}$ for $\mathbb{S}^1_d(\triangle_{\mathrm{CT}})$, suppose we assign values to all the coefficients associated with the domain points in it. These coefficients uniquely identify a spline function of $\mathbb{S}^1_d(\triangle_{\mathrm{CT}})$ because all the remaining coefficients in the local representation (9) can be deduced from the smoothness conditions (6)–(8). Therefore, any minimal determining set enables us to define a basis as follows. Let us consider the set of functions

$$\{S_{\boldsymbol{d},\triangle},\ \boldsymbol{d} \in \mathcal{M}^d_{\triangle}\}, \tag{10}$$

where $S_{\boldsymbol{d},\triangle}$ is the unique function of $\mathbb{S}^1_d(\triangle_{\mathrm{CT}})$ obtained by zeroing all the coefficients associated with the domain points in $\mathcal{M}^d_{\triangle}$ except the one related to $\boldsymbol{d}$ which is set equal to 1. By construction, the functions in (10) are linearly independent (see also [13, Theorem 5.20]) and their number agrees with the dimension of the space because of the cardinality of $\mathcal{M}^d_{\triangle}$ mentioned before. It follows that (10) is a basis for $\mathbb{S}^1_d(\triangle_{\mathrm{CT}})$; this is a so-called MDS-basis of $\mathbb{S}^1_d(\triangle_{\mathrm{CT}})$. Note that, for a given spline space, the minimal determining set is not unique and so there are several MDS-bases for a given spline space.

It is easy to see that the basis functions in (10) are locally supported: their support comprises either the star of triangles of $\triangle$ sharing a vertex, the pair of triangles of $\triangle$ having a common edge, or only a single triangle of $\triangle$. The following proposition ensures that such basis functions are uniformly bounded.

Proposition 8. *For a given triangulation $\triangle$, let $\mathcal{M}^d_\triangle$ be a minimal determining set for $\mathbb{S}^1_d(\triangle_{\mathrm{CT}})$. There exists a positive constant K depending only on the degree d and the minimal angle of $\triangle$ such that*

$$\|S_{\boldsymbol{d},\triangle}\|_\infty \le K, \quad \boldsymbol{d} \in \mathcal{M}^d_\triangle.$$

Proof. We first remark that the number of triangles surrounding a vertex of $\triangle$ and the (absolute value of the) barycentric coordinates of a point of a triangle with respect to an adjacent triangle are bounded in terms of the minimum angle of $\triangle$ (see [13, proof of Lemma 2.29]). Let $\mathcal{T}$ be a triangle of $\triangle$ belonging to the support of $S_{\boldsymbol{d},\triangle}$. We have that $(S_{\boldsymbol{d},\triangle})|_\mathcal{T}$ can be represented in the form (9) where the coefficients $c^d_{k,\mathcal{T}}$ are obtained from the value 1 associated with the domain point $\boldsymbol{d} \in \mathcal{M}^d_\triangle$ by applying the smoothness conditions (6)–(8); these conditions are simple linear relations involving barycentric coordinates of points in adjacent triangles. Therefore, denoting by $\boldsymbol{c}^d_\mathcal{T}$ the vector of these $N_\mathcal{T}$ coefficients, we obtain that $\|\boldsymbol{c}^d_\mathcal{T}\|_\infty \le K$, where K is a positive constant depending only on the degree d and the minimal angle of $\triangle$. Since the normalized simplex-splines $S^d_{k,\mathcal{T}}$ in (9) are nonnegative and form a partition of unity on $\mathcal{T}$, we get

$$\|(S_{\boldsymbol{d},\triangle})|_\mathcal{T}\|_\infty \le \|\boldsymbol{c}^d_\mathcal{T}\|_\infty \le K.$$

This concludes the proof. □

Proposition 8 implies that the proposed global basis is stable. Using the same line of arguments as the proof of [13, Theorem 5.22], one can show that for all $\boldsymbol{c}_\triangle := (c_{\boldsymbol{d},\triangle} \in \mathbb{R} : \boldsymbol{d} \in \mathcal{M}^d_\triangle)^T$,

$$K^-\|\boldsymbol{c}_\triangle\|_\infty \le \left\| \sum_{\boldsymbol{d}\in\mathcal{M}^d_\triangle} c_{\boldsymbol{d},\triangle} S_{\boldsymbol{d},\triangle} \right\|_\infty \le K^+\|\boldsymbol{c}_\triangle\|_\infty,$$

where K^- and K^+ are positive constants depending only on the degree d and the minimal angle of $\triangle$. Furthermore, from the partition of unity property of the local simplex-spline basis, we directly deduce that the global basis in (10) forms a partition of unity as well.

The approximation power of the spline space $\mathbb{S}^1_d(\triangle_{\mathrm{CT}})$ is well known and a simplified result is stated in the next proposition; see, e.g., [13]. Let $W^{d+1}_\infty(\Omega)$ be the standard Sobolev space on a domain Ω associated with the infinity norm, and let

$$|u|_{d+1,\infty} := \max_{a+b=d+1} \|D^a_x D^b_y u\|_\infty.$$

Proposition 9. *Let $\triangle$ be a given triangulation of a convex domain Ω, and denote its mesh size by h. For every function $u \in W^{d+1}_\infty(\Omega)$, there exists a spline $s \in \mathbb{S}^1_d(\triangle_{\mathrm{CT}})$ such that*

$$\|u - s\|_\infty \le K'\, h^{d+1}\, |u|_{d+1,\infty},$$

where K' is a positive constant depending only on the degree d and the minimal angle of $\triangle$.

Note that the basis construction has no influence on this approximation result.

4. Numerical examples

In this section, we numerically illustrate the performance of the considered C^1 spline spaces by means of three examples. We first study two linear problems. Given a target function $u \in L^2(\Omega)$, we aim to approximate it in the least-squares sense (Section 4.1) and as the Galerkin solution of a Poisson equation (Section 4.2). Then, we address a semilinear elliptic equation (Section 4.3). We consider four different target functions $u^{(i)}$, $i = 1, 2, 3, 4$, defined as follows:

$$u^{(1)}(x, y) = \sin(2\pi xy), \tag{11}$$

$$u^{(2)}(x, y) = \sin(7\pi(1 - x)(1 - y)), \tag{12}$$

$$u^{(3)}(x, y) = 16x(1 - x)y(1 - y)\cos(16\pi(x - 0.5)^2 + (y - 0.5)^2), \tag{13}$$

$$u^{(4)}(x, y) = xy\sin(3\pi x)\sin(3\pi y). \tag{14}$$

Fig. 7 depicts the functions in (11)–(14) on the square domain $[0, 1] \times [0, 1]$. We also consider two different domains $\Omega^{(a)}$ and $\Omega^{(b)}$, which are shown in Fig. 8 together with their initial triangulations $\triangle^{(a)}$ and $\triangle^{(b)}$ (of level $l = 0$). The triangulations are subsequently refined by dyadically splitting each triangle into four smaller triangles for each new level $l > 0$. The levels $l = 1, 2, 3$ are illustrated in Fig. 9 for both domains. We look for a spline approximation in the space $\mathbb{S}^1_d(\triangle_{\mathrm{CT}})$ of the form

$$u_h(x, y) = \sum_{\boldsymbol{d}\in\mathcal{M}^d_\triangle} c_{\boldsymbol{d},\triangle} S_{\boldsymbol{d},\triangle}(x, y),$$

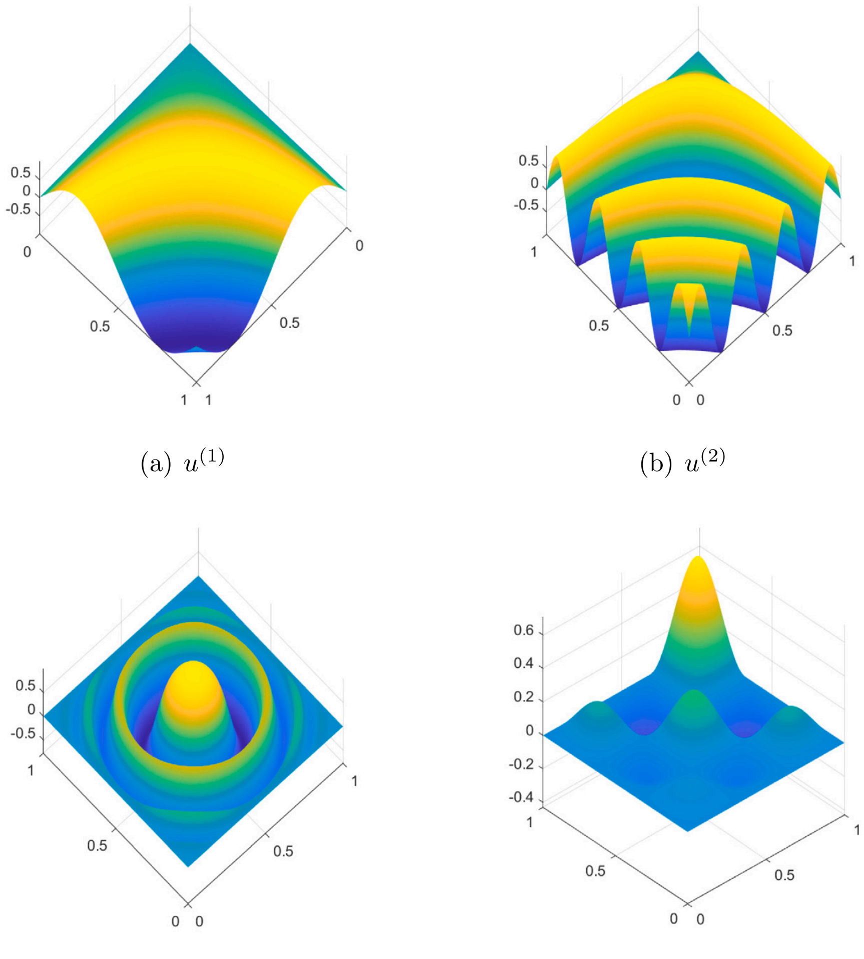

(a) $u^{(1)}$ (b) $u^{(2)}$

(c) $u^{(3)}$ (d) $u^{(4)}$

Fig. 7. Target functions $u^{(i)}$, $i = 1, 2, 3, 4$ on $[0, 1] \times [0, 1]$ defined in (11)–(14).

where $\triangle$ is the considered triangulation and $S_{d,\triangle}$ is defined in (10). The mesh size h behaves like $1/\sqrt{dof}$, where dof stands for the number of degrees of freedom. The optimal error convergence rate in the space $\mathbb{S}^1_d(\triangle_{\mathrm{CT}})$ is $\mathcal{O}(h^{d+1})$; see Proposition 9.

The integrals are numerically computed by means of triangular Gaussian quadrature rules on each subtriangle of the partition. The number of quadrature nodes are chosen to have exact integration of the involved polynomial functions.

4.1. Example 1: Least-squares problem

Given a function $u \in L^2(\Omega)$, the least-squares approximation in the space $\mathbb{S}^1_d(\triangle_{\mathrm{CT}})$ is defined as the solution of

$$\arg\min_{s\in\mathbb{S}^1_d(\triangle_{\mathrm{CT}})} \int_\Omega (u - s)^2 \, \mathrm{d}\Omega.$$

Fig. 10 shows the infinity-norm errors obtained when approximating the four target functions $u = u^{(i)}$, $i = 1, 2, 3, 4$ with respect to $\sqrt{dof}$ in the spaces $\mathbb{S}^1_3(\triangle_{\mathrm{CT}})$ and $\mathbb{S}^1_4(\triangle_{\mathrm{CT}})$. The least-squares problem is computed on the two domains $\Omega^{(a)}$ and $\Omega^{(b)}$, starting from the initial triangulations depicted in Fig. 8 and then applying dyadic refinements. In all the cases, we observe the expected optimal convergence rates, i.e., $\mathcal{O}(h^4)$ for $d = 3$ and $\mathcal{O}(h^5)$ for $d = 4$.

4.2. Example 2: Poisson problem

We consider the differential problem

$$\begin{cases} -\nabla^2 u = \mathrm{f}, & \text{in } \Omega, \\ \quad u = \mathrm{g}, & \text{on } \partial\Omega, \end{cases} \tag{15}$$

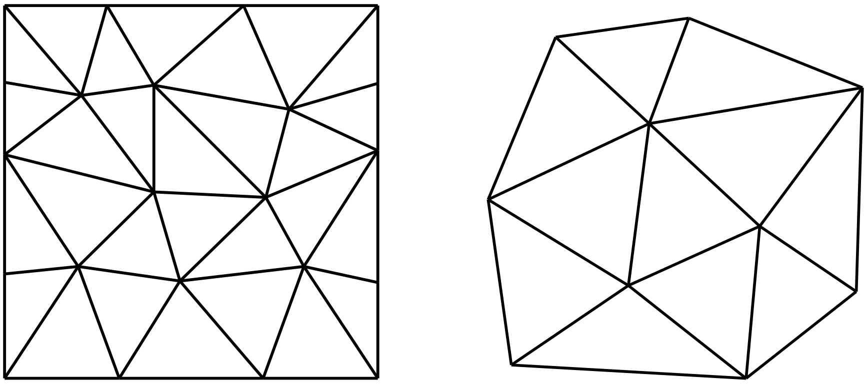

(a) $\Omega^{(a)}$ (b) $\Omega^{(b)}$

Fig. 8. Initial triangulations of the domains $\Omega^{(a)}$ and $\Omega^{(b)}$.

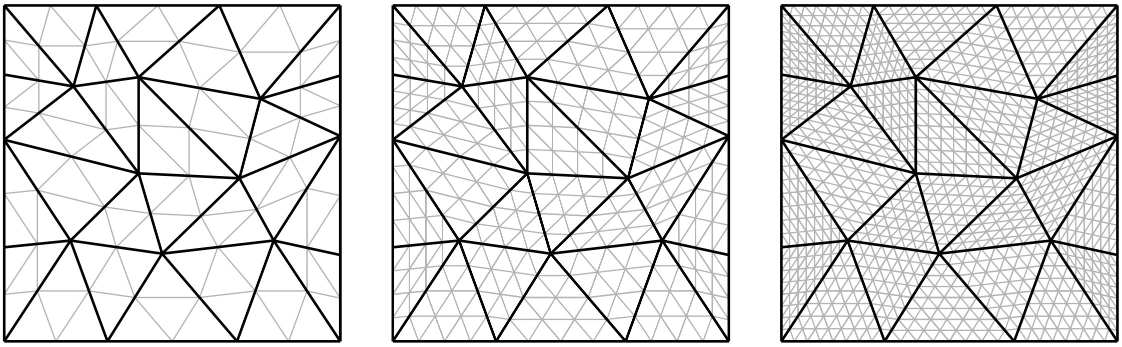

(a) $\Omega^{(a)}$

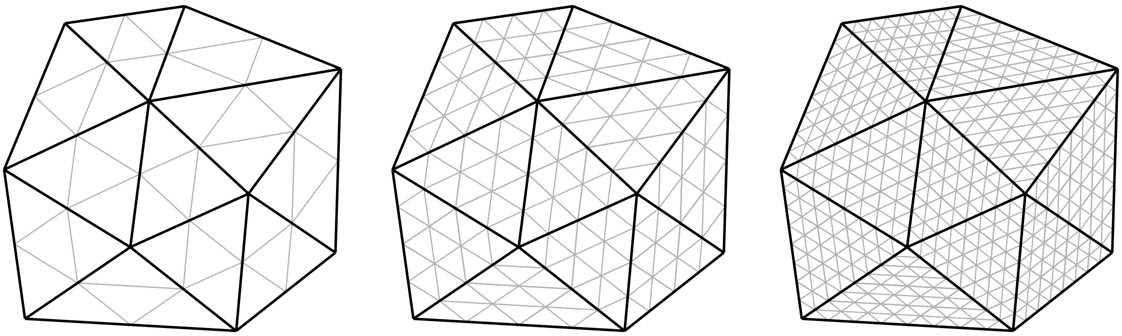

(b) $\Omega^{(b)}$

Fig. 9. Refined triangulations on the two domains $\Omega^{(a)}$ and $\Omega^{(b)}$ for refinement levels $l = 1, 2, 3$ (from left to right) starting from the initial triangulations ($l = 0$) shown in Fig. 8.

where the exact solution u is manufactured to be the four functions $u = u^{(i)}$, $i = 1, 2, 3, 4$ defined in (11)–(14) on the two domains $\Omega^{(a)}$ and $\Omega^{(b)}$ depicted in Fig. 8. The functions f, g are chosen accordingly. Fig. 11 shows the infinity-norm errors of the Galerkin approximations in the spaces $\mathbb{S}_3^1(\triangle_{\mathrm{CT}})$ and $\mathbb{S}_4^1(\triangle_{\mathrm{CT}})$, starting from the initial triangulations depicted in Fig. 8 and then applying dyadic refinements. In all the cases, we observe the expected optimal convergence rates, i.e., $\mathcal{O}(h^4)$ for $d = 3$ and $\mathcal{O}(h^5)$ for $d = 4$.

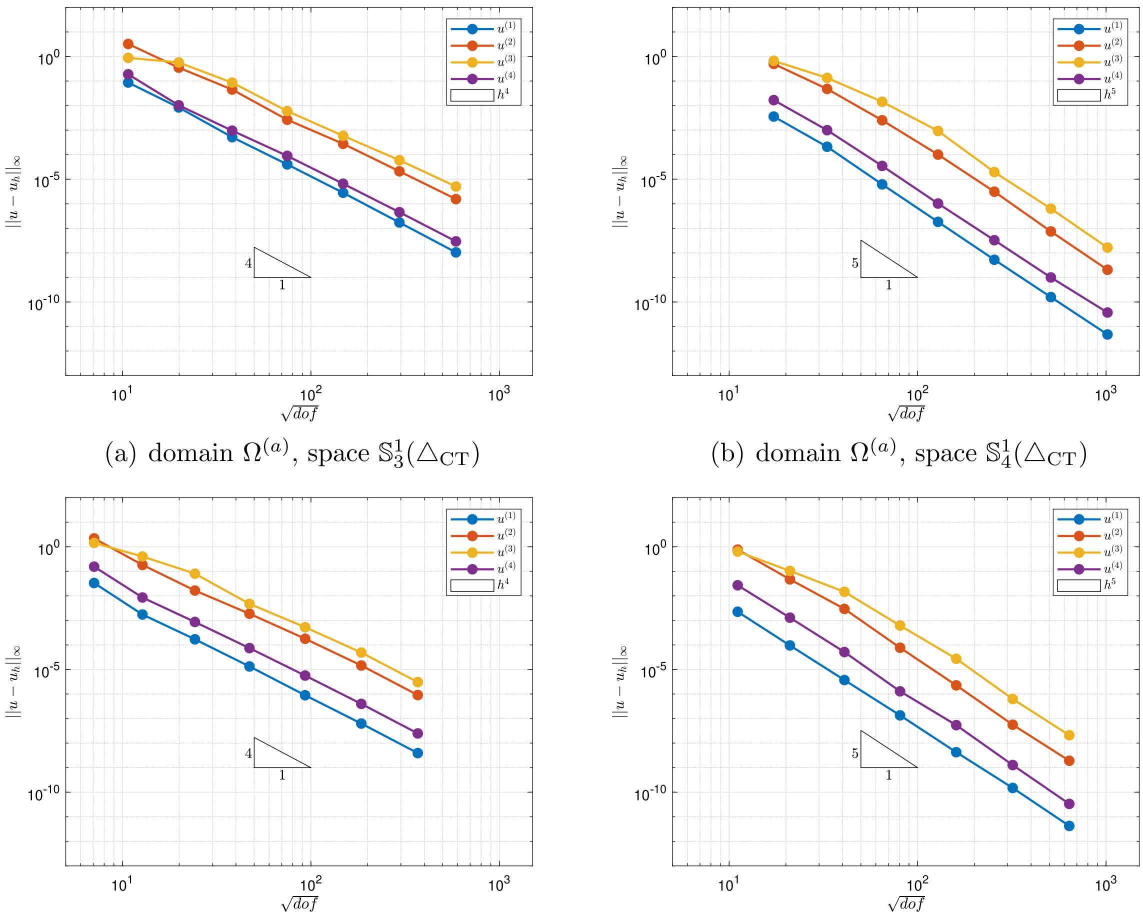

(a) domain $\Omega^{(a)}$, space $\mathbb{S}_3^1(\triangle_{\mathrm{CT}})$ (b) domain $\Omega^{(a)}$, space $\mathbb{S}_4^1(\triangle_{\mathrm{CT}})$

(c) domain $\Omega^{(b)}$, space $\mathbb{S}_3^1(\triangle_{\mathrm{CT}})$ (d) domain $\Omega^{(b)}$, space $\mathbb{S}_4^1(\triangle_{\mathrm{CT}})$

Fig. 10. (Example 1: Least-squares problem) Error in infinity norm, measured on a 100×100 grid, versus $\sqrt{dof}$ between the target functions $u^{(i)}$, $i = 1, 2, 3, 4$ defined in (11)–(14) and the least-squares approximations in the spline spaces $\mathbb{S}_3^1(\triangle_{\mathrm{CT}})$ and $\mathbb{S}_4^1(\triangle_{\mathrm{CT}})$ computed on the domains $\Omega^{(a)}$ and $\Omega^{(b)}$ depicted in Fig. 8 and refined as in Fig. 9 for the first levels.

4.3. Example 3: Semilinear elliptic problem

We consider the differential problem given by

$$\begin{cases} -\nabla^2 u = u^2 + \mathrm{f}, & \text{in } \Omega, \\ \quad u = \mathrm{g}, & \text{on } \partial\Omega, \end{cases} \tag{16}$$

where the exact solution u is manufactured to be the four functions $u = u^{(i)}$, $i = 1, 2, 3, 4$ defined in (11)–(14) on the two domains $\Omega^{(a)}$ and $\Omega^{(b)}$ depicted in Fig. 8. The functions f, g are chosen accordingly. The approximation is computed by an iterative method starting with $u_0 \equiv 0$ on Ω. Then, for $n = 0, 1, \ldots$, we compute u_{n+1} as the Galerkin solution of

$$\begin{cases} -\nabla^2 u_{n+1} = u_n^2 + \mathrm{f}, & \text{in } \Omega, \\ \quad u_{n+1} = \mathrm{g}, & \text{on } \partial\Omega. \end{cases}$$

We observe a fast convergence, therefore a few iterations are sufficient. In Fig. 12, we depict the error of the approximations $u_{h,n}$ computed on the two triangulations $\triangle^{(a)}$ and $\triangle^{(b)}$ shown in Fig. 8 and their refinements as in the previous examples. In order to reach the optimal convergence rates on the finer meshes, we use $n = 10$ iterations of the iterative method. On the coarse meshes ($l < 5$), the same accuracy can be obtained with $n = 5$.

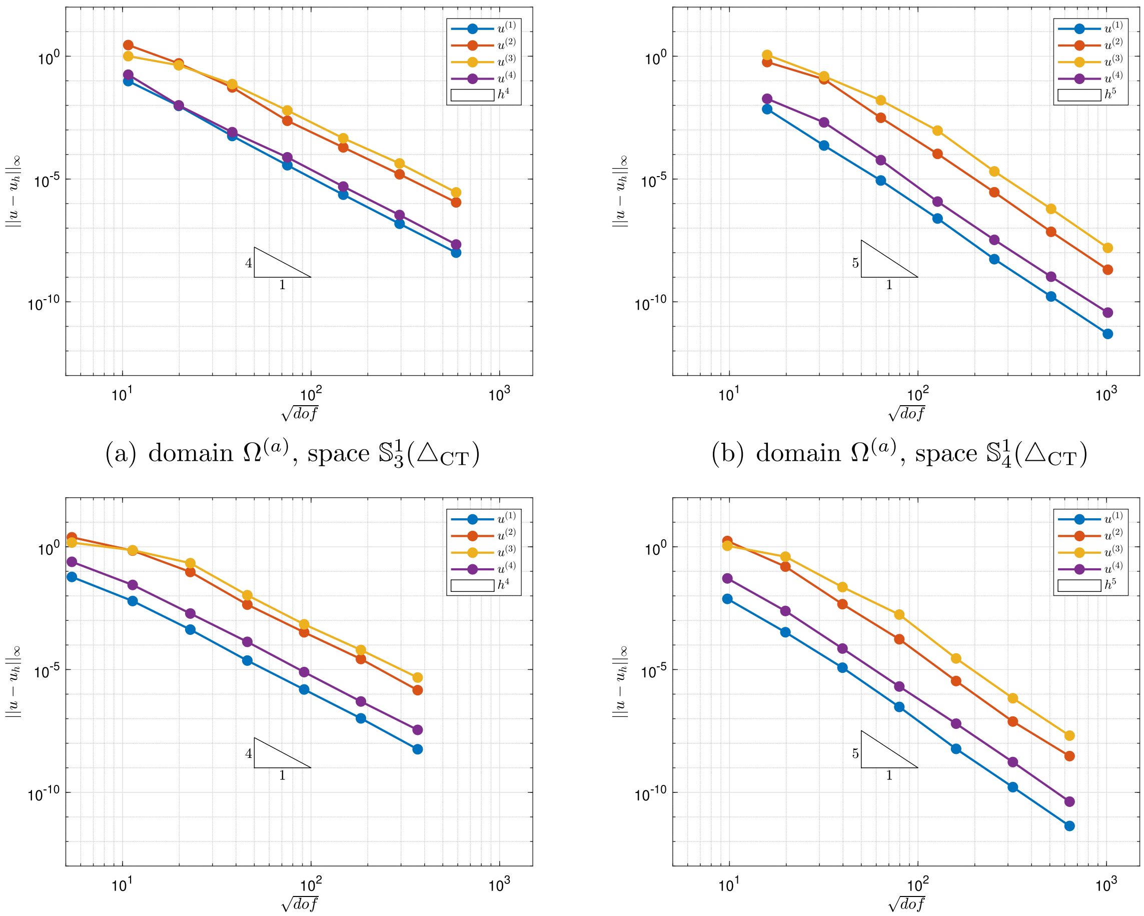

(a) domain $\Omega^{(a)}$, space $\mathbb{S}_3^1(\triangle_{\mathrm{CT}})$ (b) domain $\Omega^{(a)}$, space $\mathbb{S}_4^1(\triangle_{\mathrm{CT}})$

(c) domain $\Omega^{(b)}$, space $\mathbb{S}_3^1(\triangle_{\mathrm{CT}})$ (d) domain $\Omega^{(b)}$, space $\mathbb{S}_4^1(\triangle_{\mathrm{CT}})$

Fig. 11. (Example 2: Poisson problem) Error in infinity norm, measured on a 100 × 100 grid, versus $\sqrt{dof}$ between the exact solutions $u^{(i)}$, $i = 1,2,3,4$ defined in (11)–(14) and the Galerkin approximations in the spline spaces $\mathbb{S}_3^1(\triangle_{\mathrm{CT}})$ and $\mathbb{S}_4^1(\triangle_{\mathrm{CT}})$ computed for problem (15) on the domains $\Omega^{(a)}$ and $\Omega^{(b)}$ depicted in Fig. 8 and refined as in Fig. 9 for the first levels.

5. Conclusion

In this paper, we have investigated the (normalized) simplex-spline basis $\mathcal{S}^d$ developed in [23] for the family of C^1 spline spaces of degree $d \geq 3$ defined on the Clough–Tocher split $\mathcal{T}_{\mathrm{CT}}$ of a triangle $\mathcal{T}$ in $\mathbb{R}^2$. The split $\mathcal{T}_{\mathrm{CT}}$ is obtained by connecting the barycenter of $\mathcal{T}$ to its three vertices. The basis $\mathcal{S}^d$ consists of two types of simplex-splines: firstly Bernstein polynomials with domain points on the edges of $\mathcal{T}$ and secondly certain simplex-splines with at least one knot at the barycenter. These simplex-splines are nonnegative and form a partition of unity on $\mathcal{T}$. They also allow for simple C^1 smoothness conditions across the common edge between two adjacent triangles.

By exploiting the above properties of the simplex-spline basis and the concept of minimal determining sets, we have built a basis for any C^1 spline space of degree $d \geq 3$ defined on the Clough–Tocher refinement $\triangle_{\mathrm{CT}}$ of a general triangulation $\triangle$. The considered space contains the polynomial space of degree d and has optimal approximation power, i.e., the distance to a smooth function is $\mathcal{O}(h^{d+1})$, where h is the mesh size. We have numerically illustrated the performance of the spline spaces of degrees $d = 3,4$ by means of three examples: we have tested them in the least-squares method for function approximation and in the Galerkin method for solving linear and semilinear elliptic problems. In all the tests, the expected optimal convergence rates have been observed.

The integrals were numerically computed by means of triangular Gaussian quadrature rules on each subtriangle of the partition. This approach is not optimal, however, because the inherent smoothness of the splines is not taken into account; see [31,32] and references therein. The development of ad hoc quadrature rules might be an interesting task for future research. There are already rules available for the integration of splines of degree $d = 3r$ and smoothness C^{2r-1} on the Clough–Tocher split [32,33]. In the context of the Galerkin method, it is also of interest to develop specific weighted quadrature rules as in [31].

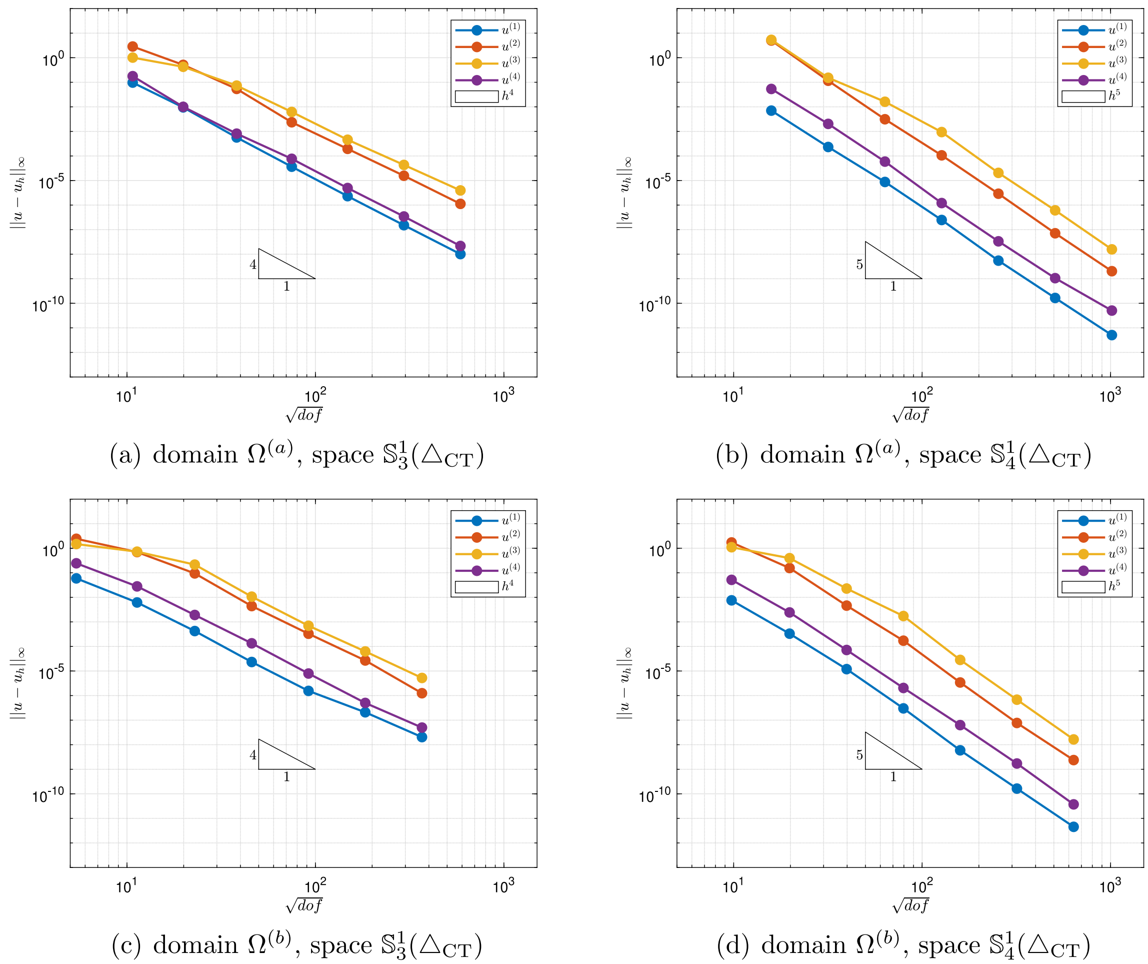

Fig. 12. (Example 3: Semilinear elliptic problem) Error in infinity norm, measured on a 100×100 grid, versus $\sqrt{dof}$ between the exact solutions $u^{(i)}$, $i = 1, 2, 3, 4$ defined in (11)–(14) and the Galerkin approximations in the spline spaces $\mathbb{S}_3^1(\triangle_{\mathrm{CT}})$ and $\mathbb{S}_4^1(\triangle_{\mathrm{CT}})$ computed for problem (16) on the domains $\Omega^{(a)}$ and $\Omega^{(b)}$ depicted in Fig. 8 and refined as in Fig. 9 for the first levels.

The simplex-spline basis is not only available for the Clough–Tocher split of a triangle in $\mathbb{R}^2$, but has actually been proposed for the more general Alfeld split of a simplex in any spatial dimension [23]. This suggests a valuable avenue for subsequent research: an expansion of the presented investigation towards simplicial partitions in higher spatial dimensions.

CRediT authorship contribution statement

Jean-Louis Merrien: Formal analysis, Methodology, Software, Writing – original draft, Writing – review & editing. **Francesca Pelosi:** Writing – review & editing, Visualization, Validation, Software, Formal analysis. **Maria Lucia Sampoli:** Formal analysis, Methodology, Software, Writing – original draft, Writing – review & editing. **Hendrik Speleers:** Formal analysis, Methodology, Software, Writing – original draft, Writing – review & editing.

Declaration of competing interest

The authors declare that they have no known competing financial interests or personal relationships that could have appeared to influence the work reported in this paper.

Acknowledgments

The authors are grateful to the CIRM (Centre International de Rencontres Mathématiques) for the Research in Residence support (No 3246). F. Pelosi, M.L. Sampoli, and H. Speleers are members of the research group GNCS (Gruppo Nazionale per il Calcolo Scientifico) of INdAM (Istituto Nazionale di Alta Matematica) and acknowledge support by a GNCS project (CUP E53C24001950001).

H. Speleers is partially supported by the MUR Excellence Department Project MatMod@TOV (CUP E83C23000330006) awarded to the Department of Mathematics of the University of Rome Tor Vergata, by the Department of Mathematics of the University of Rome Tor Vergata through the Project METRO (CUP E83C25000630005), by a Project of Relevant National Interest (PRIN) under the National Recovery and Resilience Plan (PNRR) funded by the European Union – Next Generation EU (CUP E53D23017910001), and by the Italian Research Center in High Performance Computing, Big Data and Quantum Computing (CUP E83C22003230001).

References

[1] G.E. Farin, Curves and Surfaces for CAGD: A Practical Guide, Morgan Kaufmann, 2002.
[2] H. Prautsch, W. Boehm, M. Paluszny, Bézier and B-Spline Techniques, Springer-Verlag, Berlin, 2002.
[3] J.A. Cottrell, T.J.R. Hughes, Y. Bazilevs, Isogeometric Analysis: Toward Integration of CAD and FEA, John Wiley and Sons, 2009.
[4] T.J.R. Hughes, J.A. Cottrel, Y. Basilev, Isogeometric analysis: CAD, finite elements, NURBS, exact geometry and mesh refinement, Comput. Methods Appl. Mech. Engrg. 194 (2005) 4135–4195.
[5] J.A. Evans, Y. Bazilevs, I. Babuška, T.J.R. Hughes, n-Width and sup-infs, and optimality ratios for the k-version of the isogeometric finite element method, Comput. Methods Appl. Mech. Engrg. 198 (2009) 1726–1741.
[6] E. Sande, C. Manni, H. Speleers, Sharp error estimates for spline approximation: Explicit constants, n-widths, and eigenfunction convergence, Math. Models Methods Appl. Sci. 29 (2019) 1175–1205.
[7] M.R. Dörfel, B. Jüttler, B. Simeon, Adaptive isogeometric analysis by local h-refinement with T-splines, Comput. Methods Appl. Mech. Engrg. 199 (2010) 264–275.
[8] T.W. Sederberg, J. Zheng, A. Bakenov, A. Nasri, T-splines and T-NURCCs, ACM Trans. Graph. 22 (2003) 477–484.
[9] C. Giannelli, B. Jüttler, S.K. Kleiss, A. Mantzaflaris, B. Simeon, J. Špeh, THB-splines: An effective mathematical technology for adaptive refinement in geometric design and isogeometric analysis, Comput. Methods Appl. Mech. Engrg. 299 (2016) 337–365.
[10] C. Giannelli, B. Jüttler, H. Speleers, THB-splines: The truncated basis for hierarchical splines, Comput. Aided Geom. Design 29 (2012) 485–498.
[11] T. Dokken, T. Lyche, K.F. Pettersen, Polynomial splines over locally refined box-partitions, Comput. Aided Geom. Design 30 (2013) 331–356.
[12] K.A. Johannessen, T. Kvamsdal, T. Dokken, Isogeometric analysis using LR B-splines, Comput. Methods Appl. Mech. Engrg. 269 (2014) 471–514.
[13] M.-J. Lai, L.L. Schumaker, Spline Functions on Triangulations, Cambridge Univ. Press, Cambridge, 2007.
[14] J. Grošelj, M. Knez, Generalized C^1 Clough–Tocher splines for CAGD and FEM, Comput. Methods Appl. Mech. Engrg. 395 (2022) 114983.
[15] J. Grošelj, H. Speleers, Extraction and application of super-smooth cubic B-splines over triangulations, Comput. Aided Geom. Design 103 (2023) 102194.
[16] N. Jaxon, X. Qian, Isogeometric analysis on triangulations, Comput.-Aided Des. 46 (2014) 45–57.
[17] F. Pelosi, C. Giannelli, C. Manni, M.L. Sampoli, H. Speleers, Splines over regular triangulations in numerical simulation, Comput.-Aided Des. 82 (2017) 100–111.
[18] H. Speleers, C. Manni, F. Pelosi, M.L. Sampoli, Isogeometric analysis with Powell–Sabin splines for advection-diffusion-reaction problems, Comput. Methods Appl. Mech. Engrg. 221-222 (2012) 132–148.
[19] C. Manni, T. Sorokina, Bernstein–Bézier form and its role in studying multivariate splines, in: M. Lanini, et al. (Eds.), Approximation Theory and Numerical Analysis Meet Algebra, Geometry, Topology, in: Springer INdAM Series, vol. 60, Springer, 2024, pp. 45–70.
[20] E. Cohen, T. Lyche, R.F. Riesenfeld, A B-spline-like basis for the Powell–Sabin 12-split based on simplex splines, Math. Comp. 82 (2013) 1667–1707.
[21] T. Lyche, C. Manni, H. Speleers, Construction of C^2 cubic splines on arbitrary triangulations, Found. Comput. Math. 22 (2022) 1309–1350.
[22] T. Lyche, J.-L. Merrien, Simplex-splines on the Clough–Tocher element, Comput. Aided Geom. Design 65 (2018) 76–92.
[23] T. Lyche, J.-L. Merrien, H. Speleers, A C^1 simplex-spline basis for the Alfeld split in $\mathbb{R}^s$, Comput. Aided Geom. Design 117 (2025) 102412.
[24] P.G. Ciarlet, Sur l'élément de Clough et Tocher, RAIRO – Anal. Numér. 8 (1974) 19–27.
[25] R.W. Clough, J.L. Tocher, Finite element stiffness matrices for analysis of plate bending, in: Proceedings of the Conference on Matrix Methods in Structural Mechanics, Wright-Patterson A.F.B., Ohio, 1965, pp. 515–545.
[26] J. Douglas, T. Dupont, P. Percell, R. Scott, A family of C^1 finite elements with optimal approximation properties for various Galerkin methods for 2nd and 4th order problems, RAIRO – Anal. Numér. 13 (1979) 227–255.
[27] H. Speleers, A normalized basis for reduced Clough–Tocher splines, Comput. Aided Geom. Design 27 (2010) 700–712.
[28] C.A. Micchelli, On a numerically efficient method for computing multivariate B-splines, in: W. Schempp, K. Zeller (Eds.), Multivariate Approximation Theory, Birkhäuser Verlag, Basel, 1979, pp. 211–248.
[29] A. Kolesnikov, T. Sorokina, Multivariate C^1-continuous splines on the Alfeld split of a simplex, in: G.E. Fasshauer, L.L. Schumaker (Eds.), Approximation Theory XIV, in: Springer Proceedings in Mathematics & Statistics, vol. 83, Springer, 2014, pp. 283–294.
[30] L.L. Schumaker, Computing bivariate splines in scattered data fitting and the finite-element method, Numer. Algorithms 48 (2008) 237–260.
[31] S. Eddargani, T. Lyche, C. Manni, H. Speleers, Quadrature rules for C^1 quadratic spline finite elements on the Powell–Sabin 12-split, Comput. Methods Appl. Mech. Engrg. 430 (2024) 117196.
[32] S. Eddargani, C. Manni, H. Speleers, Quadrature rules for splines of high smoothness on uniformly refined triangles, Math. Comp. 95 (2026) 321–338.
[33] J. Kosinka, M. Bartoň, Gaussian quadrature for C^1 cubic Clough–Tocher macro-triangles, J. Comput. Appl. Math. 351 (2019) 6–13.